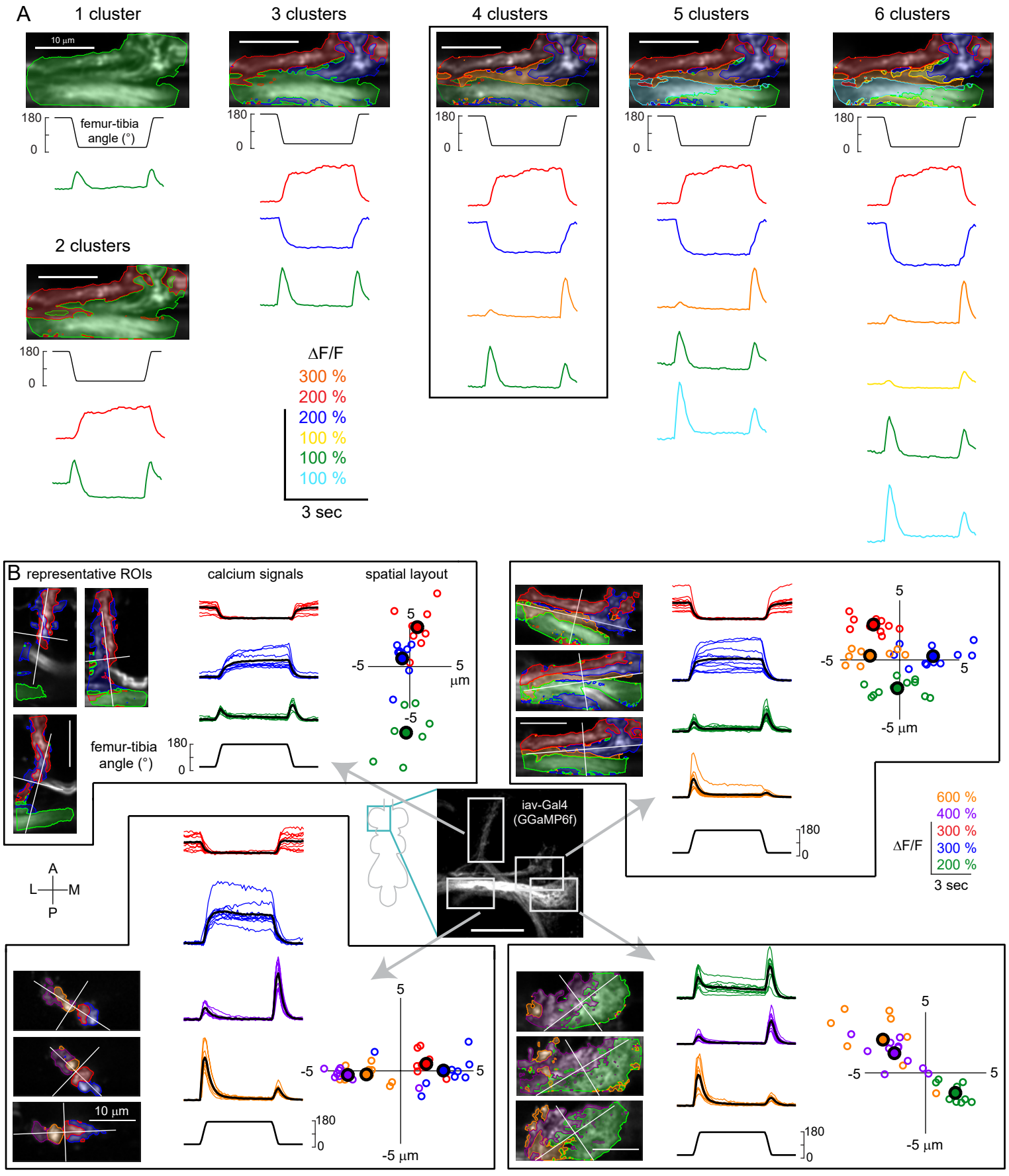

Figure S1, related to Figures 1 and 2. Example of cluster analysis and population responses for opposite swing stimuli. A. Cluster selection for the example data in Figure 1G-H. The different panels illustrate results from specifying different numbers of clusters. We increased the cluster number until we found a minimum number of nonredundant clusters (see Methods for details). **B.** Same as Figure 2, but for swing stimuli in the opposite direction (extension followed by flexion). Clustering on these data produces similar results to those in Figure 2.

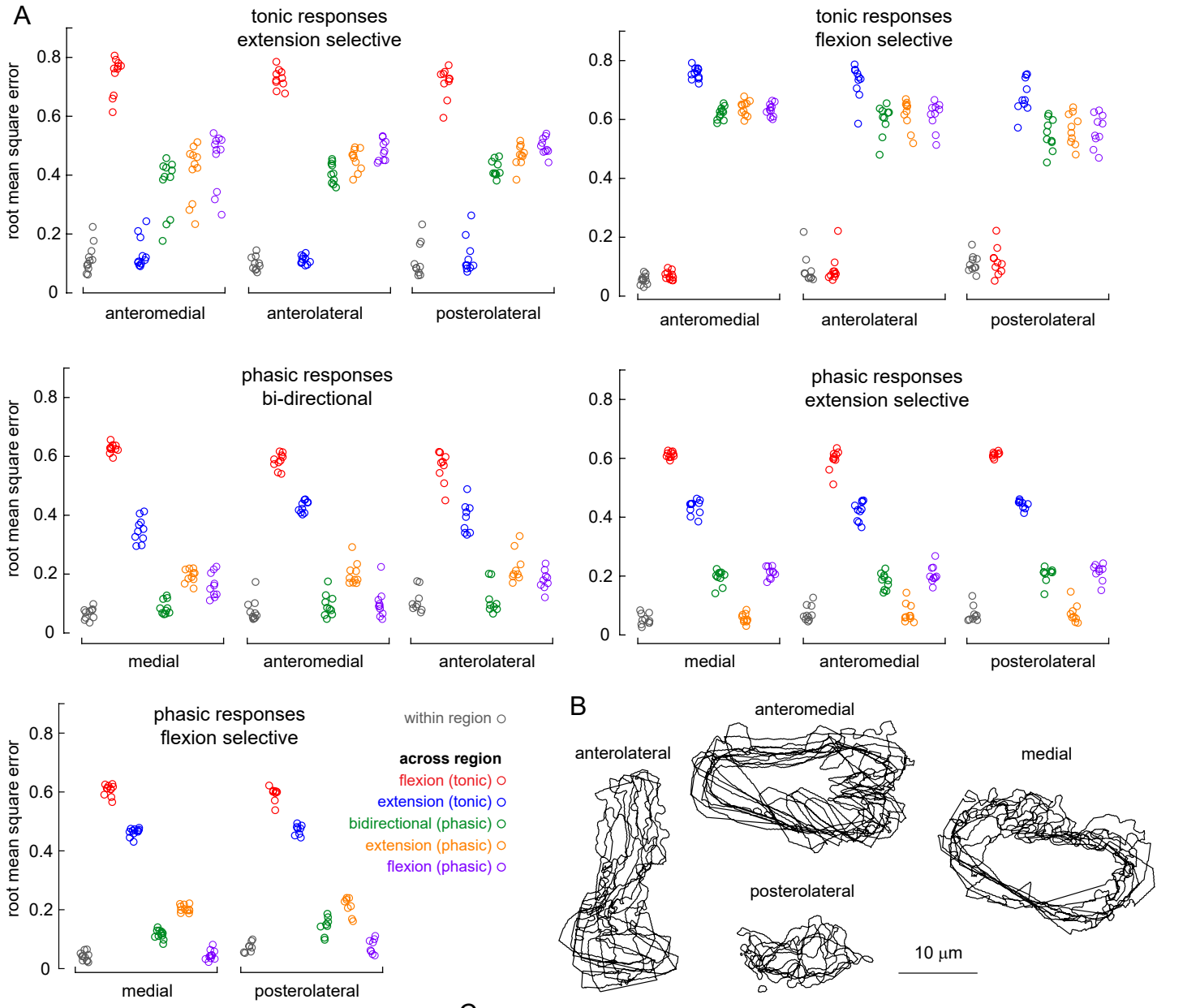

Figure S2, related to Figure 2. Additional quantification of population responses. A. For calcium signals shown in Figure 2, we computed the root mean square error from each fly to the average signal across flies, both within individual regions (grey: against the same response class) and across all regions (colors: against all response classes). **B.** Outlines of pixels containing GCaMP6f fluorescence in recordings at each location from different flies (responses shown in Figure 2). To align recordings from different flies, we rotated the images in each fly as described in the Figure 2 legend. Anterolateral, n = 10; anteromedial, n = 11; posterolateral, n = 10; medial, n = 11. **C.** Polar plots showing the relative direction and distance between different response clusters recorded from the different regions of iav-Gal4 (spatial layout plots are shown in right columns of Figure 2, and the color scheme is preserved). Polar plots shaded with light red, blue, green, and purple indicate the direction and distance from the pixels that showed flexion-selective tonic responses, extension-selective tonic responses, bi-directional phasic responses, and flexion selective phasic responses, respectively. Blue, green, orange, and purple lines in each polar plot show the direction and distance to the pixels that showed extension-selective tonic responses, bidirectional phasic responses, extension-selective phasic responses, and flexion selective phasic responses, respectively. Number of response clusters are the same as in Figure 2.

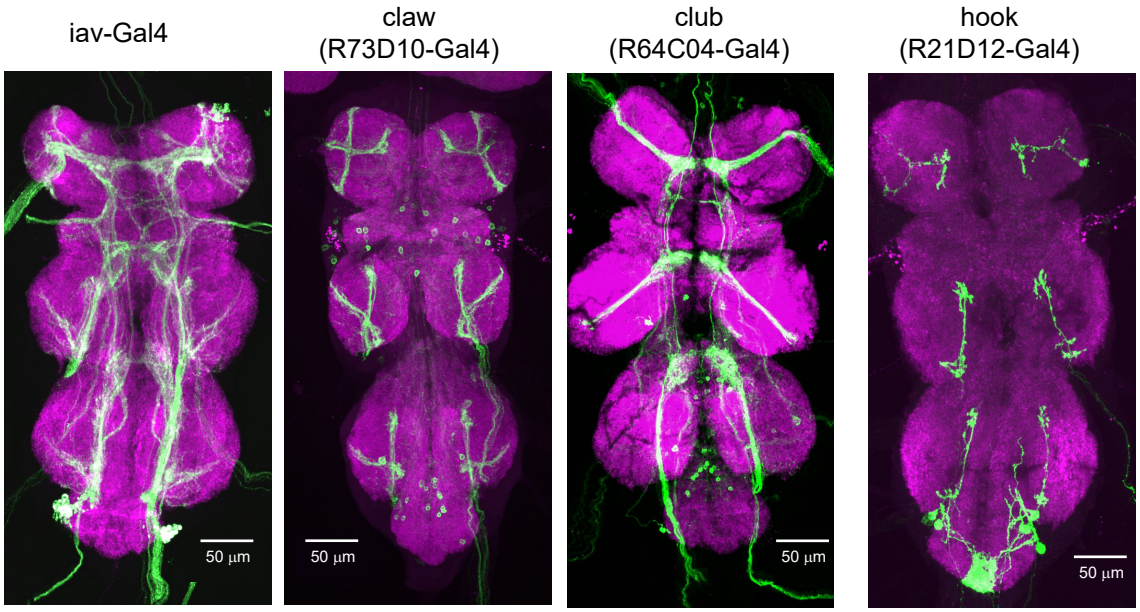

Figure S3, related to Figure 3. Anatomy of Gal4 driver lines used to label FeCO neurons. The images are the same as those in Figure 3A, but show expression in the whole VNC.

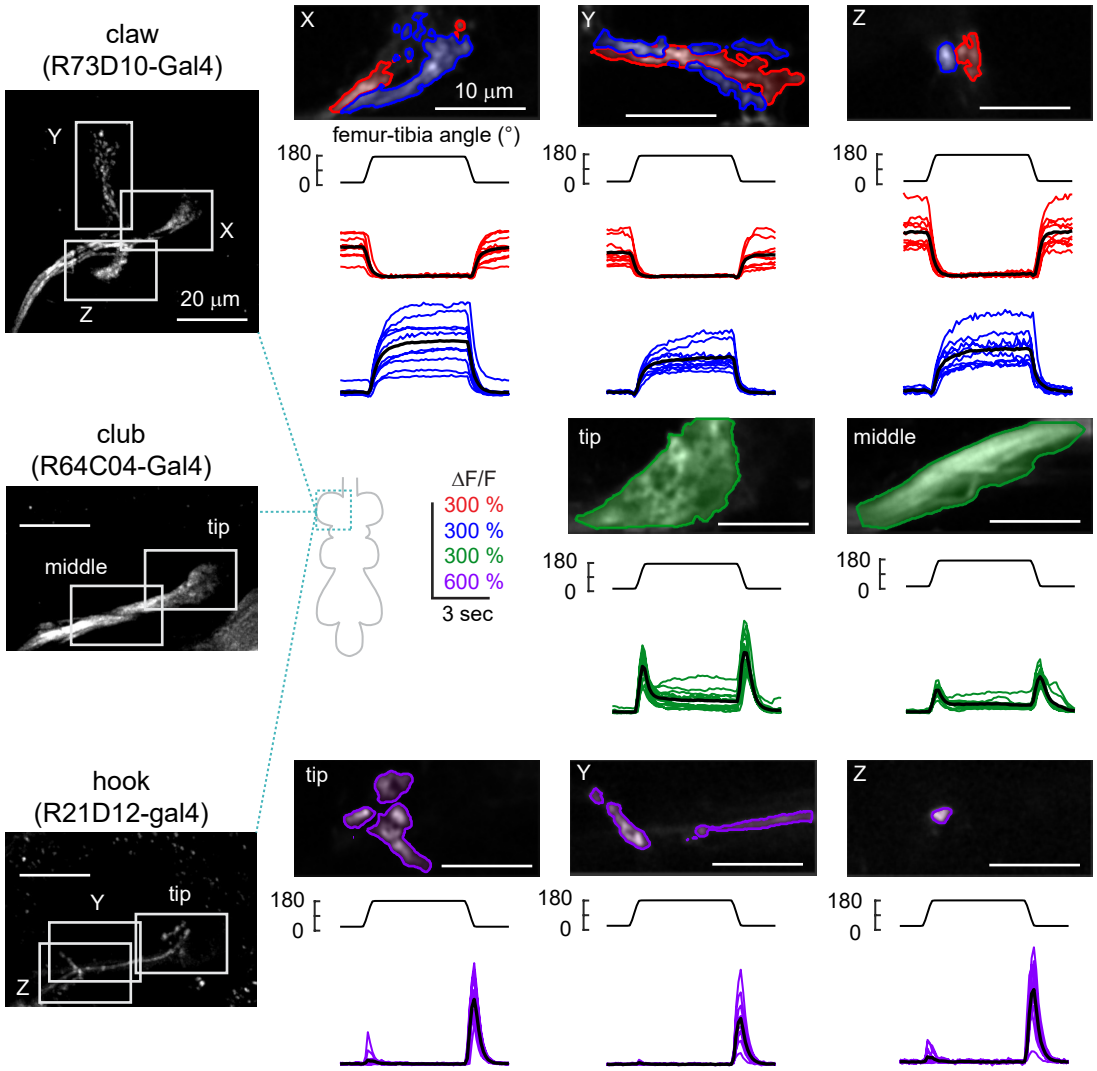

Figure S4, related to Figure 4. Responses of neurons labeled by specific Gal4 lines to swing stimuli. Same as Figure 4, but for swing stimuli in the opposite direction (extension followed by flexion). Response properties of each class of FeCO neurons are similar.

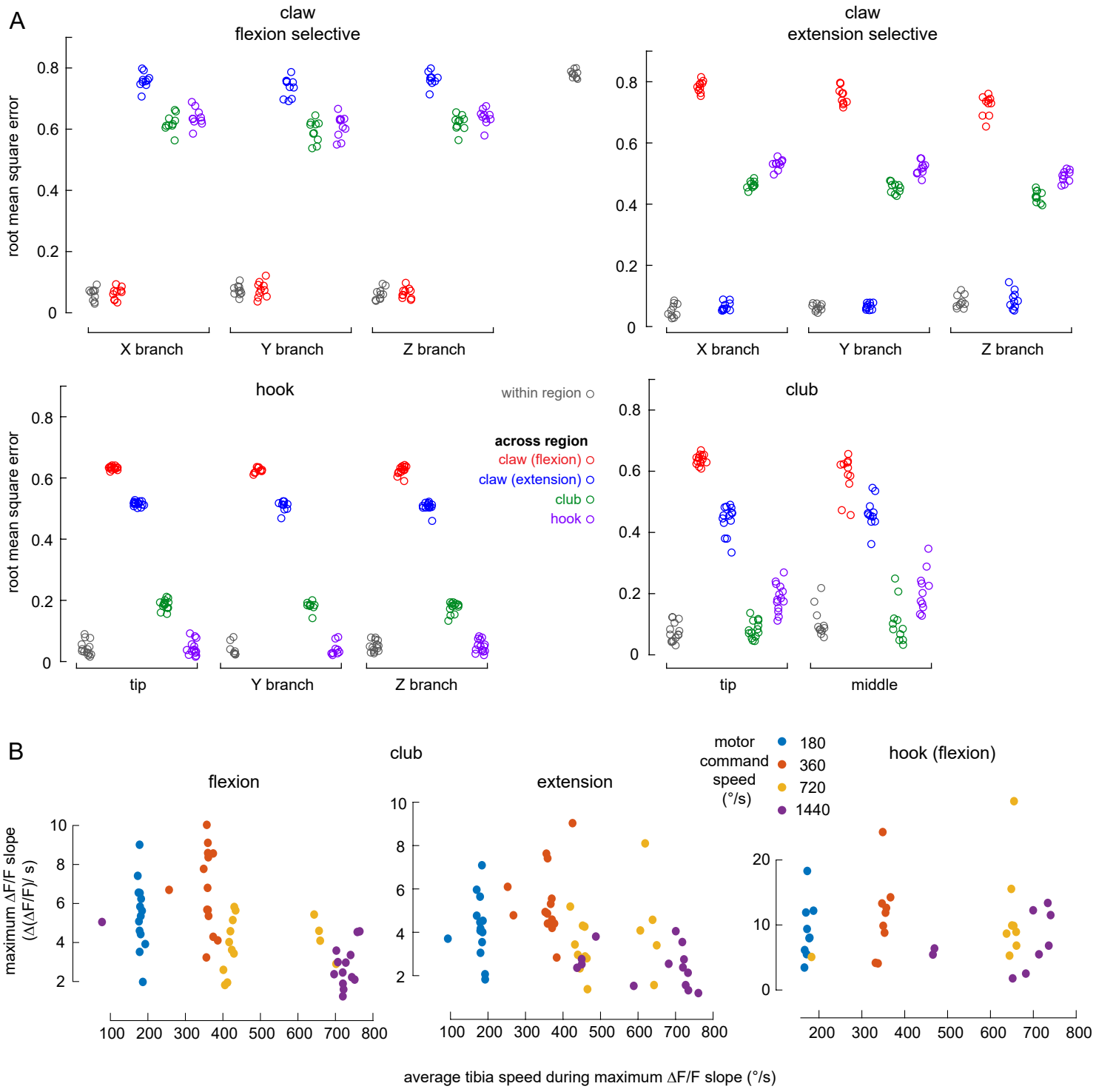

Figure S5, related to Figure 4. Additional quantification of subclass-specific responses. A. To compare response tuning across different axon projections and driver lines, we computed the root mean square error of calcium signals from each fly against the average calcium signal across flies, both within individual regions (grey: against the same response class only) and across all regions (colors: against all response classes). The response time courses for these data are shown in Figure 4. **B.** Left: Scatter plot showing the maximum slope of the ΔF/F curve for the club axons (recorded at the tip) as a function of average tibia swing speed. Each circle represents the average maximum slope of the ΔF/F curve in one fly. We calculated the average velocity of tibia movement from the frame interval in which we observed the maximum slope of the ΔF/F curve. For both flexion and the extension, n = 14 flies for all speeds. Right: Same as the left side, but for hook axons recorded at the Y branch region. Because hook neurons respond only to the flexion, we only show the plot for flexion movements. n = 9 flies for all speeds.

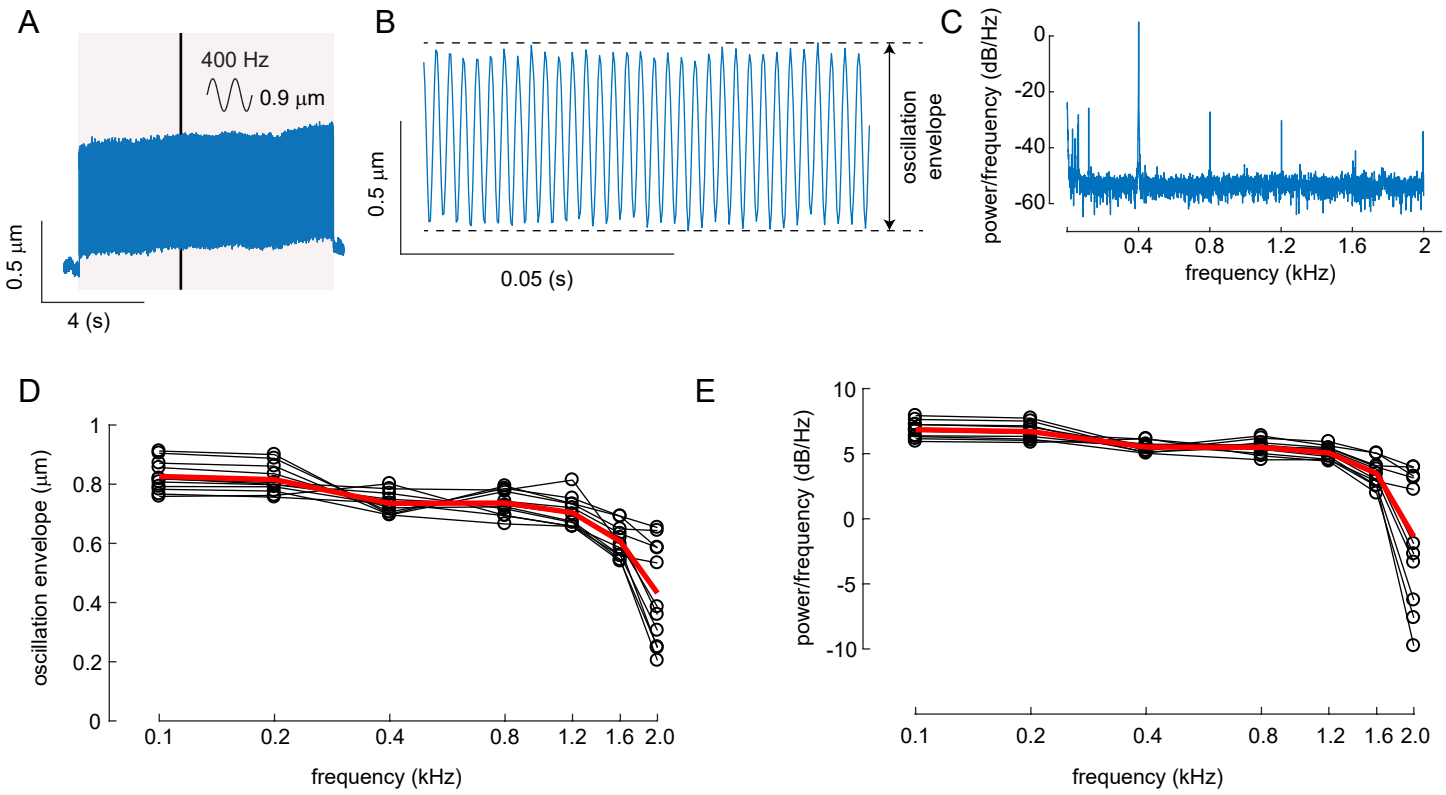

Figure S6, related to Figure 6. Calibration of vibration stimuli. A. An example tibia movement in response to a 400 Hz sine wave vibration of the piezoelectric crystal with 0.9 µm peak-to-peak amplitude. The grey shaded region indicates the duration of the piezo vibration. The black line represents the region expanded in B. **B.** An expanded view of the example tibia movement shown in A. **C.** The power spectrum of the example tibia movement shown in A. **D.** A plot showing how the oscillation envelope (as measured in B) of the tibia movement changed as we varied the command frequency of the piezoelectric crystal. Black lines indicate the oscillation envelope at different frequencies (n = 11 flies). The red line represents the mean oscillation envelope at different frequencies. The peak-to-peak amplitude of the piezo vibration was 0.9 µm for all frequencies. **E.** A plot showing how the power of the tibia vibration at the piezo command frequency changes as a function of command frequency. Black lines indicate the power of the tibia vibration at different frequencies for each fly (n = 11 flies). The red line represents the mean power of the tibia vibration at different frequencies.

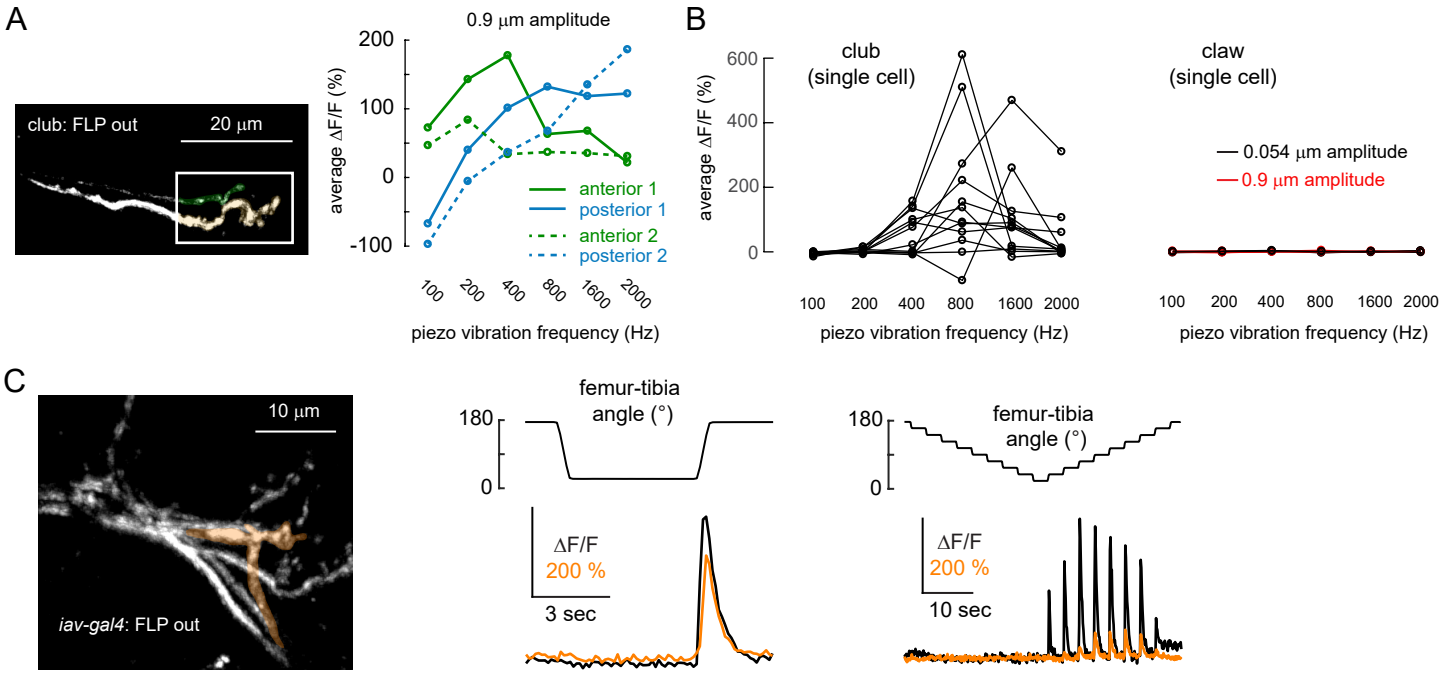

Figure S7, related to Figure 7. Examples responses of single club, claw, and extension selective phasic neurons. A. When there were axons of two club neurons, the anterior axon was tuned to lower vibration frequency compared to the posterior axon. Left: GCamp6f fluorescence in two club neurons (R64C04-Gal4), imaged on the 2-photon microscope. Right: Example frequency tuning of single club axons to 0.9 μm amplitude vibrations. Each line represents an average response from a single club axon. We calculated the average responses in the same way as in Figures 6D and 7D. **B.** Single club neurons show diverse tuning to 0.054 μm amplitude vibrations, while claw neurons do not respond to any vibrations. Left: Frequency tuning of single club axons in response to the 0.054 μm amplitude vibrations (0.9 μm responses are shown in Figure 7D). Each trace indicates the average response of one club axon (n = 12 cells from 7 flies). Right: The same as left side, but for single claw axons in response to both 0.9 μm and 0.054 μm amplitude vibrations (n = 4 cells from 4 flies). **C.** A stochastically-labeled neuron from iav-Gal4 that is directionally-selective for tibia extension. Left: GCaMP6f fluorescence in at least four axons driven by iav-Gal4, imaged on the 2-photon microscope. Orange shading indicates the axon of an extension selective phasic neuron. Middle: Responses of extension selective phasic neurons during swing motion of the tibia. Each trace shows the average calcium signal from a single extension selective phasic axon (n = 2 cells from 2 flies). The response of the axon indicated in the left image is shown in orange. Right: The same as the middle panel but for ramp-and-hold motion of the tibia (n = 2 cells from 2 flies).

Table S1, Table of genotypes, related to STAR Methods experimental model and subject details

Figure 1A	w[1118]; P{JFRC7-20XUAS-IVS-mCD8::GFP} attp40/+; iav-Gal4/+
Figure 1D	w[1118]; P{JFRC7-20XUAS-IVS-mCD8::GFP} attp40/+; iav-Gal4/+
Figure 1E, G	w[1118]/+; P{20xUAS-IVS-GCaMP6f} attP40 /+ ; iav-Gal4/P{w[+mc]=UAS-tdTomato}
Figure 2A-D	w[1118]/+; P{20xUAS-IVS-GCaMP6f} attP40 /+ ; iav-Gal4/P{w[+mc]=UAS-tdTomato}
Figure 3 A	w[1118]; P{JFRC7-20XUAS-IVS-mCD8::GFP} attp40/+; iav-Gal4/+ w[1118]; P{JFRC7-20XUAS-IVS-mCD8::GFP} attp40/+; P{GMR73D10-GAL4}attP2/+ w[1118]; P{JFRC7-20XUAS-IVS-mCD8::GFP} attp40/+; P{GMR64C04-GAL4}attP2/+ w[1118]; P{JFRC7-20XUAS-IVS-mCD8::GFP} attp40/+; P{GMR21D12-GAL4}attP2/+
Figure 3B	w[1118] P{y[+t7.7] w[+mC]=hs-FlpG5.PEST}attP3/ w[1118]; +/+; P{y[+t7.7] w[+mC]=10xUAS(FRT.stop)myr::smGdP-OLLAS}attP2 PBac{y[+mDint2] w[+mC]=10xUAS(FRT.stop)myr::smGdP-HA}VK00005 P{10xUAS(FRT.stop)myr::smGdP-V5-THS-10xUAS(FRT.stop)myr::smGdP-FLAG}su(Hw)attP1/ P{GMR73D10-GAL4}attP2 w[1118] P{y[+t7.7] w[+mC]=hs-FlpG5.PEST}attP3/ w[1118]; +/+; P{y[+t7.7] w[+mC]=10xUAS(FRT.stop)myr::smGdP-OLLAS}attP2 PBac{y[+mDint2] w[+mC]=10xUAS(FRT.stop)myr::smGdP-HA}VK00005 P{10xUAS(FRT.stop)myr::smGdP-V5-THS-10xUAS(FRT.stop)myr::smGdP-FLAG}su(Hw)attP1/ P{GMR64C04-GAL4}attP2 w[1118] P{y[+t7.7] w[+mC]=hs-FlpG5.PEST}attP3/ w[1118]; +/+; P{y[+t7.7] w[+mC]=10xUAS(FRT.stop)myr::smGdP-OLLAS}attP2 PBac{y[+mDint2] w[+mC]=10xUAS(FRT.stop)myr::smGdP-HA}VK00005 P{10xUAS(FRT.stop)myr::smGdP-V5-THS-10xUAS(FRT.stop)myr::smGdP-FLAG}su(Hw)attP1/ P{GMR21D12-GAL4}attP2
Figure 3C-F	P{UAS-RedStinger}3, w[1118]/w[1118]; P{lexA-2xhrGFP.nls}2b/+; Mi{Trojan-lexA:QFAD.0}ChAT[MI04508-TlexA:QFAD.0]/ P{GMR73D10-GAL4}attP2 P{UAS-RedStinger}3, w[1118]/ w[1118]; P{lexA-2xhrGFP.nls}2b/+; Mi{Trojan-lexA:QFAD.0}ChAT[MI04508-TlexA:QFAD.0]/ P{GMR64C04-GAL4}attP2 P{UAS-RedStinger}3, w[1118]/ w[1118]; P{lexA-2xhrGFP.nls}2b/+; Mi{Trojan-lexA:QFAD.0}ChAT[MI04508-TlexA:QFAD.0]/ P{GMR21D12-GAL4}attP2
Figure 3G	w[1118]; P{JFRC7-20XUAS-IVS-mCD8::GFP} attp40/+; P{GMR73D10-GAL4}attP2/+ w[1118]; P{JFRC7-20XUAS-IVS-mCD8::GFP} attp40/+; P{GMR64C04-GAL4}attP2/+ w[1118]; P{JFRC7-20XUAS-IVS-mCD8::GFP} attp40/+; P{GMR21D12-GAL4}attP2/+
Figure 4A	w[1118]/+; P{20xUAS-IVS-GCaMP6f} attP40 /+; P{GMR73D10-GAL4}attP2/P{w[+mc]=UAS-tdTomato}
Figure 4B	w[1118]/+; P{20xUAS-IVS-GCaMP6f} attP40 /+; P{GMR64C04-GAL4}attP2/P{w[+mc]=UAS-tdTomato}
Figure 4C	w[1118]/+; P{20xUAS-IVS-GCaMP6f} attP40; P{GMR21D12-GAL4}attP2/P{w[+mc]=UAS-tdTomato}
Figure 5A, D-E	w[1118]/+; P{20xUAS-IVS-GCaMP6f} attP40 /+; P{GMR73D10-GAL4}attP2/P{w[+mc]=UAS-tdTomato}
Figure 5B	w[1118]/+; P{20xUAS-IVS-GCaMP6f} attP40 /+; P{GMR64C04-GAL4}attP2/P{w[+mc]=UAS-tdTomato}
Figure 5C	w[1118]/+; P{20xUAS-IVS-GCaMP6f} attP40; P{GMR21D12-GAL4}attP2/P{w[+mc]=UAS-tdTomato}
Figure 6B, E-G	w[1118]/+; P{20xUAS-IVS-GCaMP6f} attP40 /+; P{GMR64C04-GAL4}attP2/P{w[+mc]=UAS-tdTomato}
Figure 6D	w[1118]/+; P{20xUAS-IVS-GCaMP6f} attP40 /+; P{GMR64C04-GAL4}attP2/P{w[+mc]=UAS-tdTomato} w[1118]/+; P{20xUAS-IVS-GCaMP6f} attP40 /+; P{GMR73D10-GAL4}attP2/P{w[+mc]=UAS-tdTomato} w[1118]/+; P{20xUAS-IVS-GCaMP6f} attP40 /+; P{GMR21D12-GAL4}attP2/P{w[+mc]=UAS-tdTomato}
Figure 7A-D	w[1118] pBPhsFlpPESTOpt attp3/ 20X-UAS>myrTopHat2>Syn21-opGcamp6f-p10 (attp8); +/sp; P{GMR64C04-GAL4}attP2/+
Figure 7E-H	w[1118] pBPhsFlpPESTOpt attp3/ 20X-UAS>myrTopHat2>Syn21-opGcamp6f-p10 (attp8); +/sp; P{GMR73D10-GAL4}attP2/+